ECS Solid State Letters, **3** (10) R49-R52 (2014)
2162-8742/2014/3(10)/R49/4/$31.00 © The Electrochemical Society

Effects of Position of Exciton-Blocking Layer on Characteristics of Blue Phosphorescent Organic Light-Emitting Diodes

Sang Ho Rhee,[a] Chang Su Kim,[b] Myungkwan Song,[b] Kwun-Bum Chung,[c] and Seung Yoon Ryu[a,z]

[a]*Department of Information Display, Sunmoon University, Tangjeong-myeon, Asan, Chungnam 336-708, South Korea*
[b]*Advanced Functional Thin Films Department, Korea Institute of Materials Science (KIMS), Seongsangu, Changwon 641-831, South Korea*
[c]*Division of Physics and Semiconductor Science, Dongguk University, Seoul 100-715, South Korea*

In this study, we systematically examined the effects of the position of the exciton- blocking layer (EBL) in blue phosphorescent organic light-emitting diodes. The EBL was located either in the front and/or the rear of the emission layer (EML), and its effects to the device performances and electroluminescence spectra were investigated. The width and location of the recombination zone related to the triplet exciton quenching occurred in the devices with/without a front- or rear-EBL resulted in an optical micro-cavity effect in the EL spectrum at approximately 500 nm. The EBLs provided the direct, extra path of charge carriers from the hole transport layer (HTL)/electron transport layer (ETL) to the ETL/HTL through EML, resulting that the device operating voltage did not increase. The device with both front- and rear-placed EBLs exhibited the highest device performance, as triplet exciton quenching did not occur in it at the interface between the HTL/ETL and the EML.
 [DOI: 10.1149/2.0041410ssl]

Manuscript submitted May 19, 2014; revised manuscript received July 10, 2014. Published July 29, 2014.

It is believed that organic light-emitting diodes (OLEDs)[1–22] have great potential for use in next-generation flat panel displays and solid state lighting, owing to their ultra thin, flexible, and transparent nature and because they can be fabricated at low costs through simple solution-based processes. Phosphorescent OLEDs (PHOLEDs) are high-efficiency devices that make use of both singlet and triplet excitons. However, they tend to exhibit poor long-term stabilities.[1–6,8–10] One reason for their poor long-term device performance is the so-called "triplet exciton quenching" in the recombination zone (RZ).[13,14] Triplet excitons are generated at the interface between the emission layer (EML) and the hole-transport layer (HTL)/electron-transport layer (ETL) and diffuse into the adjacent layers, where they are eventually quenched.[1–13] In case of blue PHOLEDs, iridium-(III) bis-[(4,6-difluorophenyl)-pyridinato-N,C$^{2'}$] picolinate (FIrpic) is usually used as the dopant and *N,N′*-dicarbazolyl-3,5-benzene (mCP) as the host.[3–6] If *N,N*-bis-(1-naphthyl)-*N,N′*-diphenyl-1,1′-biphenyl-4,4′diamine (NPB) is employed as the HTL material, triplet excitons can diffuse from the EML to the HTL and undergo quenching, because NPB has a lower triplet bandgap (2.3 eV)[4,6–8] that those of FIrpic (2.7 eV)[1,4] and mCP (2.9 eV).[1,4–6] The triplet exciton diffusion length can be estimated up to 100 nm with excited state lifetime of μs order, which sufficiently diffused to adjacent layers.[1] That is why the selecting the proper exciton-blocking layer (EBL) material such that it exhibits the desirable triplet bandgap is essential for preventing triplet exciton quenching in order to improve device performance.[6–9]

In terms of the transfer of excitation energy to excitons, it is also considered that the molecules of dopants in the EML also play the role of charge traps for electrons and holes, acting as recombination centers and thereby generating excitons and increasing the operating voltage when the doping ratio is as low as 1∼3 weight percent (wt%).[11,12] However, the excessive doping ratio of 5∼20 wt% might enhance the device performance, decreasing the operation voltage because both holes and electrons can be directly injected from the HTL and the ETL into the EML dopant molecules, which act as exciton recombination centers.[13–15] If a large energy barrier exists between the HTL/ETL and the EML host or if the energy gap between the highest occupied molecular orbital (HOMO) and the lowest unoccupied molecular orbital (LUMO) of the host/dopant is too wide, charge trapping can occur.[11,12]

The placement of a mCP EBL in the front and/or rear of the EML such that its bandgap aligns properly can affect the width and location of the RZ, resulting in improved device efficiency and controllable color coordinates in PHOLEDs.[6–9,16–18] In this study, we investigated the correlation between the formation of the RZ and the device performance for different locations of the EBL in blue PHOLEDs.

Experimental

To fabricate the blue PHOLEDs, first, indium tin oxide (ITO) glass substrates were cleaned with deionized water, acetone, and isopropanol under sonication at 40 kHz. Then, the substrates were subjected to an ultraviolet-ozone (UVO) treatment to remove any contaminating organics and to increase the ITO work function. 1,4,5,8,9,11-hexaazatriphenylene-hexacarbonitrile (HAT-CN)[21,22] (60 nm) as the hole-injection layer (HIL) and NPB (30 nm) as the HTL were deposited under high vacuum (∼10^{-7} Torr). mCP doped with 10 wt% FIrpic was used as the EML material (30 nm), and mCP was used for the EBL (2.5 nm), which was placed in the front and/or the rear of the EML. 2,9-dimethyl-4,7-diphenyl-1,10-phenanthroline (BPhen) was deposited as the ETL (25 nm); it exhibits an electron mobility of ∼2×10^{-4} cm/V s,[17] which might be not compatible with the carrier mobility of ∼6.9×10^{-2} cm/V s for HAT-CN[16,21] in terms of the good charge balance in EML.[23,24] Finally, LiF/Al (1 nm/130 nm) as the dipole layer and the cathode mirror were deposited using a shadow mask in a high-vacuum chamber; the cathode had an area of 4 mm^2. The current density-luminance-voltage characteristics and electroluminescence (EL) spectra of the devices were obtained using a Keithley 2400 voltmeter and a Minolta CS-1000 spectrometer, respectively.

Results and Discussion

The device structures and energy level diagrams for the blue PHOLEDs fabricated with the EBL placed in the front and at the rear of the EML are shown in Figs. 1a and 1b, respectively. The triplet energies of the various layers are illustrated in Fig. 1b; these were 2.9 eV for the mCP layer,[1,4–6] 2.7 eV for the FIrpic layer,[1,4] and 2.5 eV for the BPhen layer.[5]

The current density-voltage, luminance-voltage, current efficiency-luminance, and power efficiency-luminance characteristics of the four PHOLEDs in which the EBL was placed in different locations are shown in Figs. 2a, 2b, 2c, and 2d, respectively. The structures of the four devices were as follows. Device 1: ITO/HAT-CN (60 nm)/NPB (30 nm)[common structure I]/mCP:FIrpic (30 nm;10%)[B-EML]/BPhen (25 nm)/LiF (1 nm)/Al (130 nm)[common structure II]; device 2: common structure I/B-EML/mCP (2.5 nm) [EBL]/common structure II; device 3: common structure I/EBL/B-EML/common structure II, and device 4: common structure I/EBL/B-EML/EBL/ common structure II.

[z]E-mail: justie74@sunmoon.ac.kr

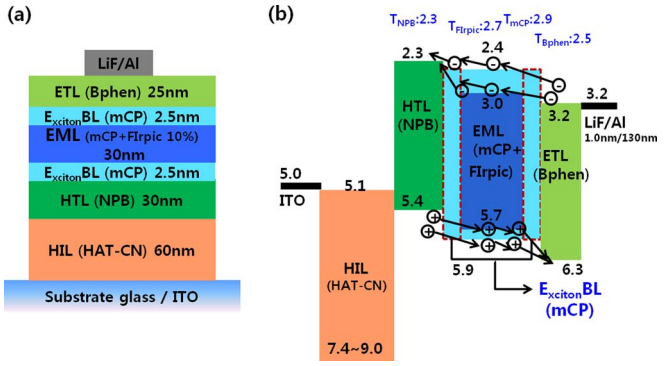

Figure 1. (a) Schematic of the device structure and (b) energy level diagrams on the various PHOLEDS with front- and/or rear-placed EBLs. [T_A = triplet energy level for A].

The current densities of all the four devices are shown in Fig. 2a. It is likely that the differences in the current densities were caused by the differences in the placement of their EBL, which resulted in different energy band alignments. In case of device 1, the current density of device 1 was worse than that of the other devices. If the heavy doping ratio more than 10% for FIrpic in EML is used, carriers could be injected into FIrpic directly and the operation voltage might be decreased.[13–15] Moreover, the triplet excitons generated at the interface between the EML and the HTL/ETL in the absence of an EBL diffused into the NPB HTL and the BPhen ETL; this was because the triplet energy was lower than that in the case of FIrpic. The exitons were eventually quenched in the HTL and the ETL. It was found that this led to a decrease in the luminance in device 1, as shown in Fig. 2b. In the absence of a front- or rear-placed EBL, the current and power efficiencies of device 1 were low, as shown in Figs. 2c and 2d, respectively. This result suggested that a narrow RZ was formed in the EML because a significant degree of triplet exciton diffusion occurred, which consisted of triplet-triplet annihilation (TTA) and triplet-polaron annihilation (TPA) as shown in Fig. 4a.[1–13] Actually, the RZ is generated through the whole EML regardless of the location of the EBL. The thing is that the density of excitons in RZ at the interface with HTL/ETL could be diluted due to the triplet energy difference between EML and the adjacent layers of HTL/ETL, following the location of the EBL.

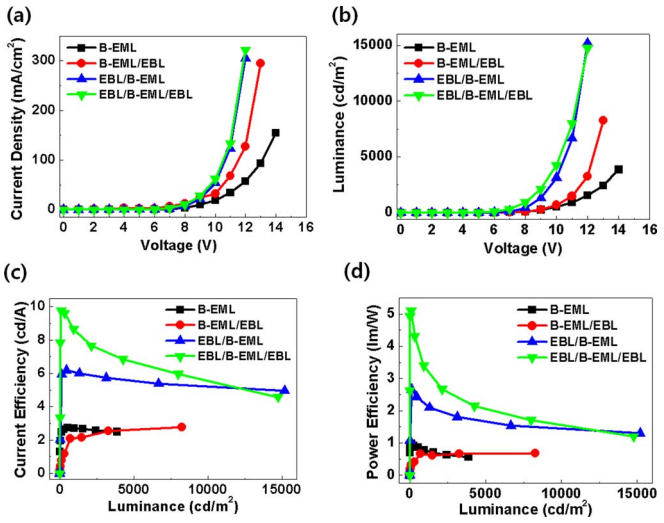

Figure 2. Performances of the various PHOLEDs: (a) current density vs. voltage, (b) luminance vs. voltage, (c) current efficiency vs. luminance, and (d) power efficiency vs. luminance.

In case of device 2, the current density was higher than that of device 1, because the rear EBL was located between the EML and the BPhen ETL; electrons were injected into the channel between the EML host and the ETL, given the LUMO energy level, as shown in Fig. 1b. The energy barrier between the NPB HTL and the EML host for the LUMO was just 0.1 eV and similar to that for an ohmic contact. This was greatly beneficial for reducing the operating voltage. However, this also increased the operating voltage, because electrons accumulated at the interface between the rear-placed EBL and the ETL. The luminance-voltage data were also better than were those of device 1, because the decrease in the number of trap centers prevented exciton quenching between the EML and the ETL.[11,12] However, the higher electron mobility of the ETL material BPhen resulted in triplet exciton quenching at the interface between the HTL and the EML. The current and power efficiencies of device 2 were almost as same as those of device 1, owing to the high probability of triplet quenching at the interface between the NPB HTL and the EML.

The current density of device 3 was better than that of device 2; however, it did not contain a rear-EBL. Therefore, there was no electron accumulation at the interface between the EML and the ETL. The operation voltage was enhanced owing to the high electron mobility of BPhen, and a smooth channel for electron injection was generated from the front EBL to the NPB HTL owing to the energy barrier being just 0.1 eV. Hole accumulation could have occurred at the interface between the NPB HTL and the front-placed EBL for the given HOMO level. However, the electron mobility of BPhen[17] is very high. Therefore, hole injection from the EML to the BPhen ETL occurred readily because the energy barrier between the mCP host and the BPhen ETL was lower than that between the FIrpic dopant and the ETL for the HOMO. The luminance, current, and power efficiencies of device 3 were better than those of devices 1 and 2. This means that the front-placed EBL was better suited than the rear-placed one, because the electron mobility of BPhen was extremely high and triplet excitons quenching was much more pronounced at the interface between the HTL and the EML.

Even though the device 4 is thicker than device 3, the current density of device 4 was the same as that of device 3 because of the smooth carrier channel in both the front- and rear-placed EBLs; carriers were directly flown to ETL and HTL as shown in Fig. 1b, and reducing driving voltage. However, the luminance was significantly higher than that of device 3, because the front- and rear-placed EBLs blocked the quenching of triplet excitons and caused the charge to be balanced in the EML. This led to improvements in the current and power efficiencies, which were higher than those of all the other devices at low operating voltages and luminance levels. However, at high operating voltages and luminances, the current and power efficiencies were almost the same as those of device 3, because both the front- and rear-placed EBLs induced carrier accumulation, resulting in TTA and TPA[2,11,12] and preventing the charge from being balanced in the EML.[23,24]

The normalized electroluminescence (EL) spectra and the Commission Internationale de l'Eclairage (CIE) color coordinates of the four devices are shown in Fig. 3. It is known that the blue dopant FIrpic generates EL peaks at 475 and 500 nm.[3–6] All four devices exhibited efficient energy transfer from the host to the dopant, resulting in typical FIrpic-like emission peaks. There might be the chance to recombine the accumulated holes/electrons and the overflowed holes/electrons at the interface between HTL/ETL and EML in all devices. Even though it is hard to say exactly that there are peaks from NPB at 458 nm in all devices except device 1 as shown in Fig. 3 inset[6–9] because peaks from NPB at 458 nm and FIrpic 475 nm are overlapped and not easy to be distinguished. However, it indicates that low device efficiencies of device 1 and 2 are originated from exciton diffusion and quenching due to the triplet energy difference without front-/rear-EBL.[25] The peak at 420 nm in device 2 and 4 seem to be attributed to accumulated carriers and exciton in rear-EBL, from mCP. In case of device 3 with front-EBL without rear-EBL, there is no peak from mCP at 420 nm because the electrons are not accumulated between HTL and

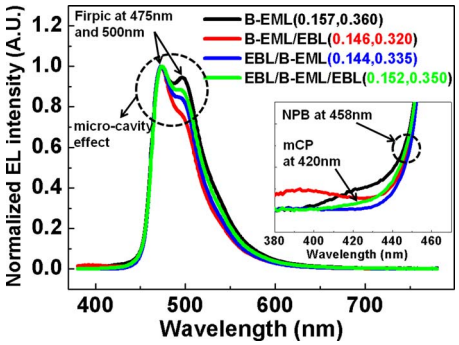

Figure 3. Normalized electroluminescence spectra and CIE color coordinates of the PHOLEDs with front- and/or rear-placed EBLs. [Inset: The magnified EL spectra from380 nm to 460 nm is shown in the inset].

EML, easily flown to HTL through front-EBL and excitons are not recombined.[25]

In the EL spectra of the devices, the intensities of the peak noticed at approximately 500 nm varied owing to the variations in the width and location of the RZ as well as variations in the total device thickness, which were attributable to differences in the placement of the EBL, as shown in Fig. 4. The variations noticed in the "shoulder peak" at approximately 500 nm were due to a micro-cavity effect, which also affected the CIE coordinates. Energy transfer is mostly conducted from mCP 420 nm peak to FIrpic 500 nm shoulder peak because the peak at 475 nm is overlapped by both mCP host and FIrpic dopant, and invariant.[4,6–9,16] The shoulder peak of FIrpic is believed to be mainly affected by energy transfer, which is related to the mico-cavity effect, following the width of RZ and the device thickness.[4,6–9,16]

Schematics of the energy level diagrams corresponding to the front- and rear-located EBLs are shown in Fig. 4. The differences in the width and locations of the RZ in the devices with the front- and rear-located EBLs determined the extent of exciton quenching, leading to the micro-cavity effect being active through the entire thickness of the devices. The excitons generated in RZ through the total EML were quenched and diluted due to the triplet energy difference between

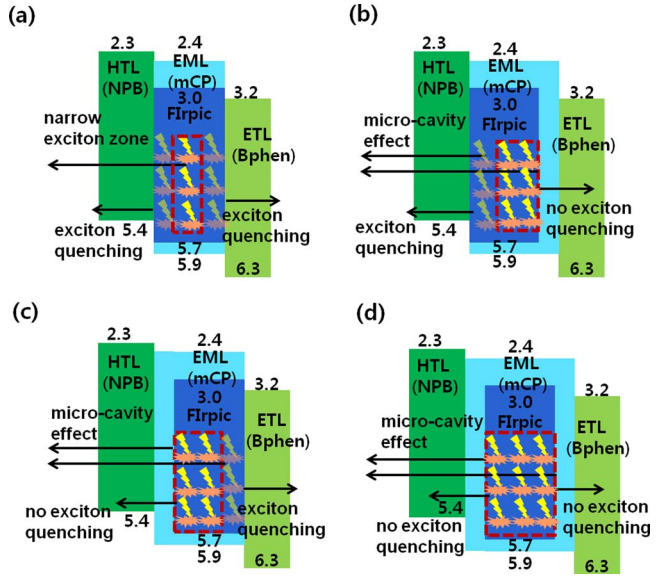

Figure 4. Schematic modeling of the different RZs and micro-cavity effects in the devices with EBLs located in different positions: (a) without an EBL, (b) with a rear-placed EBL, (c) with a front-placed EBL, and (d) with front- and rear-placed EBLs.

EML and the adjacent layers of HTL/ETL, finally seems like inducing the narrow RZ. The high electron mobility of BPhen generally results in a wide RZ;[11,12,16,17] however, the RZ of device 1 was narrow and away from the HTL and the ETL, which did not contain a front/rear EBL. This can be attributed to the triplet exciton quenching at the interface between the HTL/ETL and the EML, as shown in Fig. 4a. However, the RZ of device 2, which had only a rear-placed EBL, was localized near the ETL, and not near the HTL, as shown in Fig. 4b. This was because triplet exciton quenching occurred at the interface between the HTL and the EML. This caused the RZ to be wider than that of device 1, which had a rear-placed EBL. This induced a type of micro-cavity effect that was different from the one in the case of device 1.[16,19,20] The RZs of devices 2 and 3 were wider than that of device 1 with respect to the extent of triplet exciton quenching, because of its long diffusion lengths to the adjacent layers. This resulted in different types of micro-cavity effects, as shown in Figs. 4b and 4c, respectively. The RZ of device 4 was the widest of all; this can be attributed to the fact that triplet exciton quenching was prevented by the front/rear EBLs, resulting in a different type of micro-cavity effect in the thickest device, as shown in Fig. 4d.

The stability of device can be improved by EBL in terms of RZ stability, morphological stability, reduced charge leakage, TTA and TPA.[25] As shown in Fig. 2b, 2c and 2d, the high luminance in all devices with EBL except device 1 without EBL were showed, which means device stability was believed to be enhanced by EBL due to the good exciton confinement in EML.

Conclusions

We investigated the correlation between the placements of the EBL in PHOLEDs and device performance as it related to triplet exciton quenching and the micro-cavity effect owing to variations in the width of the RZ. Device 4, which contained both a front- and a rear-placed EBL, exhibited a higher efficiency than did the other devices, owing to the suppression of triplet exciton quenching at the interface between the HTL/ETL and the EML. In addition, the devices, in which the width of the RZ varied, exhibited the micro-cavity effect in their EL spectra at approximately 500 nm. This was because differences in the total device thickness and the width of the RZ resulted in the optical lengths being different. Elucidation of the relationship between the width of the RZ and the placement of the EBL should lead to the design and development of efficient, deep blue OLEDs.

Acknowledgments

This research was partially supported by Basic Science Research Program through the National Research Foundation of Korea (NRF) funded by the Ministry of Education, Science and Technology (NRF-2013R1A1A2A10005186) and the Pioneer Research Center Program (2013M3C1A3065525) through the National Research Foundation of Korea funded by the Ministry of Science, ICT & Future Planning.

References

1. K. S. Yook and J. Y. Lee, *Adv. Mater.*, **24**, 3169 (2012).
2. S. Reineke, K. Walzer, and K. Leo, *Phys. Rev. B*, **75**, 125328 (2007).
3. R. J. Holmes, S. R. Forrest, Y. J. Tung, R. C. Kwong, J. J. Brown, S. Garon, and M. E. Thompson, *Appl. Phys. Lett.*, **82**, 2422 (2003).
4. Q. Wang, J. Ding, D. Ma, Y. Cheng, L. Wang, X. Jing, and F. Wang, *Adv. Fun. Mater.*, **19**, 84 (2009).
5. J. W. Lee, N. Chopra, S. H. Eom, Y. Zheng, J. Xue, F. So, and J. Shi, *Appl. Phys. Lett.*, **93**, 123306 (2008).
6. J. H. Lee, J. I. Lee, K. I. Song, S. J. Lee, and H. Y. Chu, *Appl. Phys. Lett.*, **92**, 133304 (2008).
7. S. H. Kim, J. Jang, and J. Y. Lee, *Appl. Phys. Lett.*, **90**, 223505 (2007).
8. S. O. Jeon, K. S. Yook, C. W. Joo, and J. Y. Lee, *Appl. Phys. Lett.*, **94**, 013301 (2009).
9. Y. Zheng, S. Eom, N. Chopra, J. Lee, F. So, and J. Xue, *Appl. Phys. Lett.* **92**, 223301 (2008).
10. J. G. Jang, H. J. Ji, H. S. Kim, and J. C. Jeong, *Curr. Appl. Phys.*, **11**, S251 (2011).
11. X. Gong, J. C. Ostrowski, D. Moses, G. C. Bazan, and A. J. Heeger, *Adv. Fun. Mater.*, **13**, 439 (2003).

12. W. S. Jeon, T. J. Park, S. Y. Kim, R. Pode, J. Jang, and J. H. Kwon, *Org. Electron.*, **10**, 240 (2009).
13. Z. W. Liu, M. G. Helander, Z. B. Wang, and Z. H. Lu, *Appl. Phys. Lett.*, **94**, 113305 (2009).
14. Z. W. Liu, M. G. Helander, Z. B. Wang, and Z. H. Lu, *Org. Electron.*, **10**, 1146 (2009).
15. Y. F. Lv, P. C. Zhou, N. Wei, K. J. Peng, J. N. Yu, and B. Wei, *Org. Electron.*, **10**, 1146 (2009).
16. S. H. Rhee, K. B. Nam, C. S. Kim, and S. Y. Ryu., *Electronchem. solid State Lett.*, **3**, R7 (2014).
17. S. H. Rhee, K. B. Nam, C. S. Kim, M. K. Song, W. S. Cho, S. H. Jin, and S. Y. Ryu, *Electronchem. solid State Lett.*, **3**, R19 (2014).
18. J. H. Lee, J. I. Lee, J. Y. Lee, and H. Y. Chu, *Appl. Phys. Lett.*, **95**, 253304 (2009).
19. V. Bulovic, V. B. Khalfin, G. Gu, P. E. Burrows, D. Z. Garbuzov, and S. R. Forrest, *Phys. Rev. B*, **58**, 3730 (1998).
20. C.-J. Lee, Y-I. Park, J.-H. Kwon, and J.-W Park, *Bull. Korean. Chem. Soc.*, **26**, 1344 (2005).
21. S. H. Cho, S. W. Pyo, and M. C. Suh, *Synth. Met.*, **162**, 402 (2012).
22. Y. K. Kim, J. W. Kim, and Y. S. Park, *Appl. Phys. Lett.*, **94**, 063305 (2009).
23. S. W. Culligan, A. C.-A. Chen, J. U. Wallace, K. P. Klubek, C. W. Tang, and S. H. Chen, *Adv. Fun. Mater.*, **16**, 1481 (2006).
24. S.-J. Su, T. Chiba, T. Takeda, and J. Kido, *Adv. Mater.* **20**, 2125 (2008).
25. C. H. Gao, D. Y. Zhou, W. Gu, X. B. Shi, Z. K. Wang, and L. S. Liao, *Org. Electron.*, **14**, 1177 (2013).